Doppler Method for Identification of Noise Sources on Underwater Moving Target

Lingji Xu, Yixin Yang and Feng Tian
School of Marine Technology, Northwestern Polytechnical University, Xi'an
E-mail: xulingji040812@126.com Tel: +86-29-88460373

***Abstract*— According to Doppler shift of moving acoustic source signal, a method is proposed for identification of noise sources on underwater moving target with single hydrophone. The weak Doppler shift curves due to target moving are obtained by utilizing high accuracy ST-Chirp-z algorithm. Considering the sources with small frequency interval, high frequency resolution ST-ESPRIT algorithm is used to extract the Doppler shift curves. After curve smoothing with outlier removing and median filtering, the abeam time when noise sources have the nearest distance to hydrophone is estimated by least square method. Locations of multiple noise sources are obtained with the reference point of a beacon at last. The results of experiment in anechoic water tank showed the validity of this new method, and verified its high localization accuracy.**

I. INTRODUCTION

Ship-radiated noise comes from the host propulsion system, propeller, auxiliary machine system and hydrodynamic effect of ship. The stable low-frequency line spectrum caused by the reciprocating motion of the auxiliary machine carries important information of target characteristic, and it can be detected in a far distance. The noise reduction of ship is not only valuable for avoiding the detection from underwater sound equipment and the attack of underwater weapons, but also useful for improving the performance of underwater sound equipment on the ship. Therefore, the noise reduction becomes an urgent task of acoustic design of ship. However, the identification of the noise sources is the premise of noise reduction.

Identification of noise has been investigated in the past several decades, and several methods have been proposed, including coherent analysis [1], sound intensity measurement [2], acoustical holography [3], and beamforming [4]. HE et al applied the technique of acoustical holography to identification of noise sources on underwater target, and obtained some useful results [5-6]. Yet, the cost of the measuring system is too expensive due to the tremendous number of hydrophones needed. YAN used the technique of high resolution direction-finding with array to indentify the noise sources of moving target [7]. However, the result is difficult to be applied in practice due to its go-stop-go model. The passing property of the ship is still used at present [8], but the accuracy of localization is low.

In this paper, according to Doppler shift of moving acoustic sources, a new method is proposed for identification of noise sources on underwater moving target with single hydrophone. This method uses frequency estimation algorithms to extract Doppler shift curve of the moving target and obtains the abeam time of each noise sources on the target by least square algorithm, then the localization of noise sources can be known. The rest of this paper is organized as follows. We first formulate the problem and measurement model in Section II. The proposed method is then presented in Section III, and the simulation is described in Section IV. Finally, the results of the experiment are given to demonstrate the feasibility of the proposed method.

II. MEASUREMENT MODEL

The model for measuring ship-radiated noise is shown in Fig. 1, where the measured ship moves at a constant speed in the trajectory of *MN* and the measurement hydrophone is located at *S*. Because of the relative motion between the ship and the hydrophone, the line spectrum frequencies of the received signal will change with time.

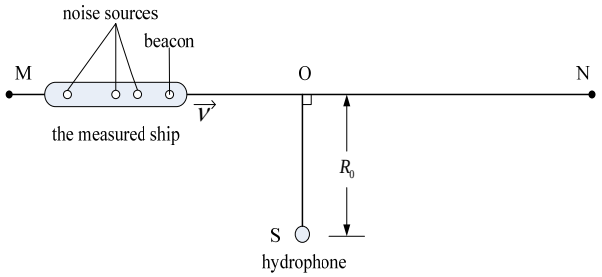

Fig. 1 Model for measuring ship-radiated noise.

The frequency of signal received by the hydrophone can be written as

$$f = \frac{c}{c + \dfrac{v^2(t-t_0)}{\sqrt{R_0^{\,2} + v^2(t-t_0)^2}}} f_0 \qquad (1)$$

here f_0 is the frequency of the source signal, v is the speed of the target, c is the sound velocity, R_0 is the abeam distance, and t_0 is the abeam time. An example of Doppler shift of single source is shown in Fig. 2.

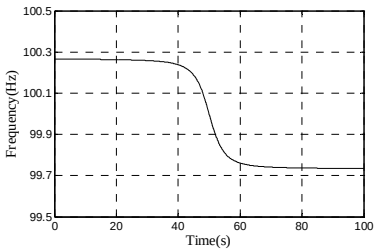

Fig. 2 Doppler shift curve of a source with v =4m/s, MN=400m, R_0 =20m, f_0 =100Hz, and c =1500m/s.

Fixing a known beacon source at the position L_c on the target, the abeam time of the beacon then can be estimated according to the Doppler shift curve of the beacon. In the same way, the abeam time of noise sources can be also obtained. Finally, the positions of each noise source on the target L_n are as follow

$$L_n = \nu\left(\hat{t}_n - \hat{t}_c\right) + L_c \tag{2}$$

where $\hat{t}_c$ and $\hat{t}_n$ represent the estimated value of the abeam time of the beacon and the noise sources respectively . This method is called Doppler method. In the next section, we will illustrate the Doppler method in detail.

III. Doppler Method

The Doppler method to identify noise sources contains three main steps. Firstly, the data received by the hydrophone is preprocessed, then Doppler shift curves are extracted by the frequency estimation algorithms, and finally the locations of acoustic sources can be obtained referring to beacon using the Doppler parameters estimated by the least square method.

A. Preprocessing

The purpose of preprocessing is to choose the line spectrum signal. After changing the data received by the hydrophone to be complex, the frequency distribution of the source signal is estimated by FFT. Then, the narrowband signal contains line spectrum can be obtained with bandpass filter, and the signal-to-noise ratio (SNR) of the signal is also improved.

B. Extracting Doppler Shift Curves

The short-time Fourier transform (STFT) is a useful algorithm for extracting Doppler shift curves [9]

$$\mathrm{STFT}_x(\omega,\tau)=\int_{-\infty}^{\infty} x(t)g(t-\tau)e^{-j\omega t}dt \tag{3}$$

here $g(t)$ is time window, and $x(t)g(t-\tau)$ is assumed to be stationary signal. It is indicated from (3) that $\mathrm{STFT}_x(\omega,\tau)$ is FFT of $x(t)$ around the particular time t .

The procedure for STFT is given as follow. The signal is first divided into overlap subsections by sliding the time window. Each subsection of the signal is then multiplied by window function to decrease sidelobe leakage produced by finite time. Finally, the time-frequency distribution of signal is obtained after FFT of each subsection of signal. The Doppler shift curves can be extracted by using the peak detection after STFFT. Since Doppler shift is weak due to the slow velocity of the target and the low frequencies of the sources, it requires large number of FFT point to get high resolution. The small varying frequency values of Doppler shift could only be observed clearly in this way.

a High Accuracy ST-Chirp-z Algorithm

The computational burden increases with the points of FFT. So, the Chirp-*z* transform is used to improve the computing efficiency. Considering *N*-point signal $x(n)$, the computation of *z*-transform on a more general contour is formulated as follow [10]

$$z_k = AW^{-k}, k = 0,1,2,\cdots,M-1 \tag{4}$$

where M is an arbitrary integer, and both A and W are arbitrary complex numbers of the form

$$\begin{cases} A = A_0 e^{j\theta_0} \\ W = W_0 e^{-j\varphi_0} \\ z_k = A_0 e^{j\theta_0} W_0^{-k} e^{-jk\varphi_0} \end{cases} \tag{5}$$

here A_0 and W_0 are real-valued constants, and φ_0 is the included angle of two adjacent analysis points. The general *z*-plane contour begins with the point $z = A$, and depending on the value of W , spirals in or out with respect to the origin.

Put z_k into the formula of *z*-transform

$$\begin{aligned} X(z_k) &= \sum_{n=0}^{N-1} x(n)[AW^{-k}]^{-n} \\ &= \sum_{n=0}^{N-1} x(n)A^{-n}W^{kn}, 0 \le k \le M-1 \end{aligned} \tag{6}$$

use the ingenious substitution

$$nk = \frac{1}{2}[n^2 + k^2 - (k-n)^2] \tag{7}$$

an apparently more unwieldy expression is produced

$$\begin{aligned} X(z^k) &= \sum_{n=0}^{N-1} x(n)A^{-n}W^{[n^2+k^2-(k-n)^2]/2} \\ &= W^{k^2/2}\sum_{n=0}^{N-1} x(n)A^{-n}W^{n^2/2}W^{-(k-n)^2/2} \end{aligned} \tag{8}$$

define

$$y(n) = x(n)A^{-n}W^{n^2/2} \tag{9}$$

and

$$h(n) = W^{-n^2/2} \tag{10}$$

use (8), (9) and (10), we get

$$X(z_k) = W^{k^2/2} \sum_{n=0}^{N-1} y(n)h(k-n)\ , 0 \le k \le M-1 \tag{11}$$

Since the algorithm enables the evaluation of the *z*-transform at M equi-angularly spaced points on contours which spiral in or out from an arbitrary starting point in the *z*-plane, the Chirp *z*-transform has a great flexibility. Combining this algorithm with STFFT, the Doppler shift curve can be extracted in arbitrary accuracy, and this modified algorithm for time-frequency analysis is called ST-Chirp-*z*.

b High Frequency Resolution ST-ESPRIT Algorithm

Due to the nonstationarity of signal caused by Doppler shift, the samples of signal used for ST-Chirp-*z* can't be too more, and this limits the frequency resolution of ST-Chirp-*z* algorithm. We can use high frequency resolution ESPRIT algorithm instead of FFT in STFFT algorithm when frequency intervals of line spectrum signals are less than Fourier threshold. Consider hydrophone output signal $x(n)$ consisting of p sinusoidal signals with Gaussian white noise

$$x(n) = \sum_{i=1}^{p} A_i \exp(j\varphi_i)\exp(j2\pi f_i n) + z(n), n = 0,1,2,\cdots,N-1 \tag{12}$$

where the amplitudes $\{A_i\}$ are real-valued positive constants, the initial phases $\{\varphi_i\}$ are independent random variables distributed uniformly on $[0, 2\pi)$, and the frequencies $\{f_i\}$ are distinct $(f_i \ne f_k, k \ne j)$. It is assumed that $\{\varphi_i\}$ and $\{z(n)\}$ are independent, and $z(n)$ is complex Gaussian white noise with zero mean and variance σ_z^2. The autocovariance matrix of $x(n)$ is given by

$$R_{xx} = \sum_{i=1}^{p} P_i \hat{e}_i \hat{e}_i^H + \sigma_z^2 I = R_{ss} + R_{zz} \tag{13}$$

here $\hat{e}_i = \left[1, \exp(j\omega_i), \cdots, \exp(j\omega_i(M-1))\right]^T, i = 1,2,\cdots,p$, and the rank of M $(M > p)$ order signal matrix R_{ss} is equal to p, so R_{ss} is a singular matrix. Let $\{\lambda_1, \cdots, \lambda_M\}$ denote the eigenvalues of R_{ss} arranged in decreasing order $(\lambda_1 \ge \lambda_2 \ge \cdots \lambda_M)$, the last $(M-p)$ eigenvalues will be zero. Now consider the eigendecomposition of R_{xx}

$$R_{xx} = \sum_{m=1}^{p} (\rho_m + \sigma_z^2)\hat{v}_m \hat{v}_m{}^H + \sum_{m=p+1}^{M} \sigma_z^2 \hat{v}_m \hat{v}_m{}^H \tag{14}$$

where $(M-p)$ small eigenvalues $\{\lambda_{p+1}, \lambda_{p+2}, \cdots, \lambda_M\}$ are equal to σ_z^2, and the space spanned by the orthonormal eigenvectors $\{\hat{v}_{p+1}, \hat{v}_{p+2}, \cdots, \hat{v}_M\}$ is called noise subspace; p big eigenvalues $\{\lambda_1, \lambda_2, \cdots, \lambda_p\}$ are called main eigenvalues, and the corresponding eigenvectors $\{\hat{v}_1, \hat{v}_2, \cdots, \hat{v}_p\}$ are main eigenvectors. It is easy to be proved that the main eigenvectors are in signal subspace [11]

$$span\{\hat{e}_1, \hat{e}_2, \cdots, \hat{e}_p\} = span\{\hat{v}_1, \hat{v}_2, \cdots, \hat{v}_p\} \tag{15}$$

Let $E = \left[\hat{e}(\omega_1), \hat{e}(\omega_2), \cdots, \hat{e}(\omega_p)\right]$, and define

$$\begin{aligned} E_1 &= [I_{M-1} \quad 0]E \\ E_2 &= [0 \quad I_{M-1}]E \end{aligned} \tag{16}$$

here I_{M-1} is the identity matrix of dimension $(M-1)\times(M-1)$. Clearly,

$$E_2 = E_1 D \tag{17}$$

with $D = \begin{bmatrix} e^{j\omega_1} & & 0 \\ & \ddots & \\ 0 & & e^{j\omega_p} \end{bmatrix}$.

Similar to (16), we can define

$$\begin{aligned} U_1 &= [I_{M-1} \quad 0]U_s \\ U_2 &= [0 \quad I_{M-1}]U_s \end{aligned} \tag{18}$$

where U_s is a matrix consisting of main eigenvectors. From (15), the following relations can be established.

$$U_s = EC \tag{19}$$

here C is uniquely nonsingular matrix. Use (16), (17), (18) and (19), to write

$$U_2 = E_2 C = E_1 DC = U_1 C^{-1} DC \tag{20}$$

define $\phi = C^{-1}DC$, from (19) and the Vandermonde structure of E, it follows that E_1 and E_2 and hence also U_1 and U_2 have full rank. Thus, the matrix ϕ is uniquely given by [12]

$$\phi = \left(U_1^* U_1\right)^{-1} U_1^* U_2 \tag{21}$$

and its eigenvalues are equal to $\left\{e^{j\omega_i}\right\}_{i=1}^{p}$. The frequencies $\{\omega_i\}$ are estimated as the angular positions of the eigenvalues of the matrix ϕ.

The modified algorithm above is called ST-ESPRIT, and it resolves the problem that time resolution and frequency resolution can't be lessen together by STFFT. Since data processing is offline, the computation burden of ST-ESPRIT is not considered here.

C. Estimation of Doppler Parameters

Actually, the Doppler shift curves extracted by frequency estimation algorithm are a set of discrete points. Least square method is used to estimate the frequency f_0 and abeam time t_0 of noise sources. Let $(f_k, t_k), k = 1, 2, \cdots, N$ denote the discrete points, and use function $f = F(t; f_0, t_0)$ to represent (1) in which the parameters v and R_0 are treated as known quantities because they can be measured in practice. Define

$$L(f_0; t_0) = \sum_{k=1}^{N} \left[F(t_k; f_0, t_0) - f_k\right]^2 \tag{22}$$

Estimate the parameters f_0 and t_0 under the restriction of the least squares criterion

$$(\hat{f}_0, \hat{t}_0) = \underset{f_0, t_0}{\mathrm{ArgMin}}\, L(f_0; t_0) \tag{23}$$

Solve the following equations

$$\begin{cases} \dfrac{\partial L(f_0; t_0)}{\partial f_0} = 0 \\ \dfrac{\partial L(f_0; t_0)}{\partial t_0} = 0 \end{cases} \tag{24}$$

then, the parameter values of $\hat{f}_0$ and $\hat{t}_0$ can be obtained.

Equation (24) is an evaluation optimizing problem. Gauss-Newton iterative algorithm can be used to find the optimum solution, and the initial value of iterative is chosen according to the predicted point of inflexion on extracted Doppler shift curve. The number of data N is a factor that affects the estimation accuracy of Doppler parameters. In practice, the complete procedure for estimating the parameters of Doppler shift is formulated as follows:

1) Choose the data in the middle of Doppler shift curves after smoothing the extracted Doppler shift curves with outlier removing and median filtering.
2) Use different windows to cut out the data obtained by step (1) under the principle that the section of symmetrical data whose middle point is the predicted point of inflexion on extracted Doppler shift curve. Then, Doppler parameters of each data are estimated by least square method.
3) Average the estimated values of the Doppler parameters.

IV. Computer Simulation

Throughout all simulation in the work, R_0 =20m, v =4m/s, c =1500m/s, the sampling time is 100s, SNR= 5dB, and SNR is defined as the ratio of signal to average noise. Fig. 3 shows the extracted Doppler shift curves of single source with different frequencies.

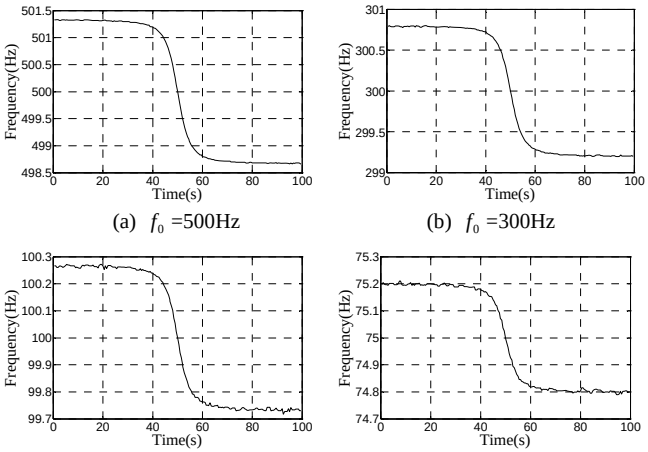

(a) f_0 =500Hz (b) f_0 =300Hz

(c) f_0 =100Hz (d) f_0 =75Hz

Fig. 3 The extracted Doppler shift curves of single source with different frequencies.

The Doppler parameters and errors of localization are listed in Table I. The results show $\hat{f}_0 < 0.01$Hz, and it can be easily known that the error of localization is less than 0.1m by using the formula $\Delta s = v\left|\hat{t}_0 - t_0\right|$.

TABLE I
Doppler Parameters and Localization Errors of Single Source with Different Frequencies

Number of signal	1	2	3	4
f_0 (Hz)	75	100	300	500
$\hat{f}_0$ (Hz)	74.9991	99.9996	299.9994	499.9997
t_0 (s)	50	50	50	50
$\hat{t}_0$ (s)	50.0204	50.0047	50.0011	49.9994
Δs (m)	0.0816	0.0188	0.0044	0.0024

Fig. 4 shows the extracted Doppler shift curves of double sources. In Fig. 4(a), the algorithm is ST-Chirp-z, while the algorithm is ST-ESPRIT in Fig. 4(b). As indicated in Fig. 4, components of signal will interfere each other when the frequency interval of two acoustic sources becomes less; and the less the interval, the greater the fluctuation of Doppler shift curve is. However, from the analysis results in Table II, it can be seen that the errors of localization are still less than 0.1m after using least square estimate.

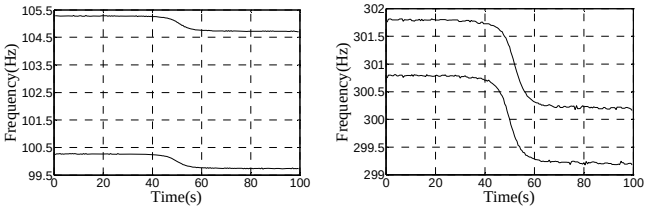

(a) $\Delta f_0 = 3\text{Hz}, \Delta t_0 = 1\text{s}$ (b) $\Delta f_0 = 1\text{Hz}, \Delta t_0 = 2\text{s}$

Fig. 4 Doppler shift curves of double sources.

Table II
Doppler Parameters and Localization Errors of Double Sources

Number of signal	1		2	
f_0 (Hz)	100	105	300	301
$\hat{f}_0$ (Hz)	100.0004	105.0009	300.0021	300.9996
t_0 (s)	50	51	50	52
$\hat{t}_0$ (s)	49.9961	50.9782	49.9826	52.0059
Δs (m)	0.0158	0.0087	0.0698	0.0238

In order to show clearly the relation between the error of localization and SNR, the single source whose frequency is equal to 100Hz is discussed in Fig. 5. It can be seen from Fig. 5(a) that the bias curve fluctuates slightly around zero, and this indicates that the Doppler method is unbiased estimate with SNR. Fig. 5(b) shows that the greater the SNR, the less the RMSE is; and the RMSE is less than 0.4m when SNR is above -10dB while the RMSE is close to zero when SNR is above 10dB.

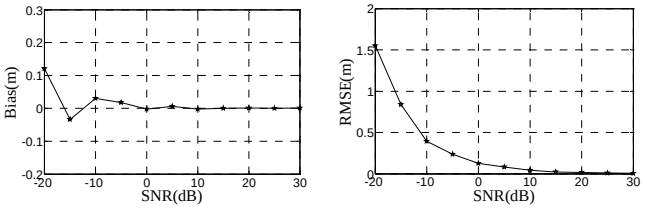

(a) The curve of Bias (b) The curve of RMSE

Fig. 5 Relation between the error of localization and SNR.

The error of localization is concerned with the frequency of line spectrum. SNR is considered to be equal to 5dB. Fig. 6(a) shows that the bias is almost equal to zero, and this result indicates that the Doppler method is unbiased estimate with frequency. It can be seen in Fig. 6(b) that the greater the frequency, the less the RMSE is; and the RMSE is less than 0.1m when frequency is above 80Hz while the RMSE is close to zero when frequency is high.

V. EXPERIMENT IN WATER TANK

In the experiment, the sampling time of analog Doppler signals produced by computer with NI PCI-6722 D/A card is 50s. It should be pointed out that the signal of double sources is composed by Doppler signals of two single sources. The SNR of each source is 5dB, and the noise is Gaussian white noise added into the signal.

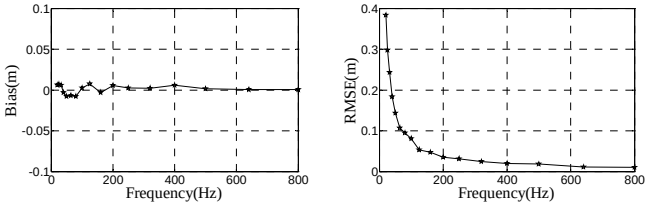

(a) The curve of Bias (b) The curve of RMSE

Fig. 6 Relation between the error of localization and value of center frequency.

Fig. 7(a) shows the recorded Doppler signal, and the Doppler shift curve extracted by ST-Chirp-*z* algorithm is shown in Fig. 7(b). It can be obtained that $\hat{f}_0 = 700.6972\text{Hz}$ and $\hat{t}_0 = 24.9848\text{s}$ by using least square method. So, it is clear that the error of localization is 0.0608m which is less than 0.1m.

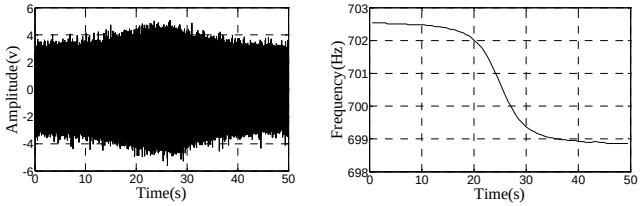

(a) The recorded acoustic signal (b) The Doppler shift curve

Fig. 7 Single acoustic source with f_0 =700.7Hz in experiment.

Fig. 8 shows the extracted Doppler shift curves of double sources with two set of data. In Fig. 8(a), the algorithm is ST-Chirp-*z*, while the algorithm is ST-ESPRIT in Fig. 8(b). The results are given in Table III.

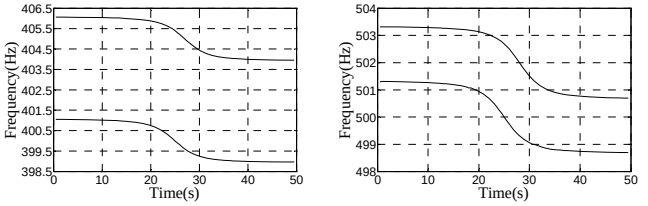

(a) $\Delta f_0 = 5\text{Hz}, \Delta t_0 = 2\text{s}$ (b) $\Delta f_0 = 2\text{Hz}, \Delta t_0 = 3\text{s}$

Fig. 8 Doppler shift curves of double sources in experiment.

Table III
Doppler Parameters and Localization Errors of Double Sources in Experiment

Number of signal	1		2	
f_0 (Hz)	400	405	500	502
$\hat{f}_0$ (Hz)	399.9973	404.9967	499.9970	501.9963
t_0 (s)	25	27	25	28
$\hat{t}_0$ (s)	24.9880	27.0203	25.0182	27.9897
Δs (m)	0.0480	0.0812	0.0728	0.0412

It can be seen from the above results of experiment that the estimate errors of frequency are less than 0.01Hz and the errors of localization are less than 0.1m when SNR is equal to 5dB. The results show that the source positions can be accurately identified by the proposed method.

VI. Conclusions

A method for identification of noise sources on underwater moving target according to the Doppler shift of tonal noise sources is proposed. The Doppler shift curves of moving acoustic sources are firstly extracted accurately by frequency estimation algorithms. Then, Doppler parameters are estimated by least square method. Locations of noise sources are identified by referring to beaconing finally. This method is easy for practice due to only using single hydrophone. Simulations are presented to demonstrate the feasibility of the proposed method, and results of experiment in anechoic tank show that the location error is less than 0.1m when SNR is equal to 5dB. Therefore, the proposed Doppler method has potential usage in practice.

Acknowledgment

This work was supported by the National Natural Science Foundation of China (10974153, 10734030) and Fundamental Research Project (973) of China.

References

[1] Chen X Z, "Progress of techniques for noise source identification," *Journal of HeFei University of Technology*, vol. 32, pp. 609-614, 2009.

[2] He Z Y, "Review of some aspects of underwater noise including its control techniques and its prospect," *Applied Acoustics*, vol. 21, pp. 26-34, 2002.

[3] Bai M R, Lin J H, "Source identification system based on the time-domain nearfield equivalence source imaging: Fundamental theory and implementation," *Journal of Sound and Vibration*, vol. 307, pp. 202-225, 2007.

[4] Chen J C et al, "Source localization and beamforming," *IEEE SP Magazine*, pp. 30-39, 2002.

[5] He Y A, He Z Y, "Full spatial transformation of sound field based on planar acoustic holography: I. Principle and algorithm," *Acta Acustica*, vol. 27, pp. 507-512, 2002.

[6] He Y A, He Z Y, "Full spatial transformation of sound field based on planar acoustic holography: II. Experiment of NAH for submerged large area planar transmitting array," *Acta Acustica*, vol. 28, pp. 45-51, 2003.

[7] Yan G H, Chen Z F, and Sun J C, "A method for localizing noise source of constant-speed target," *Journal of Northwestern Polytechnical University*, vol. 27, pp. 378-381, 2009.

[8] Wang Z C et al, *Warship noise measuring and analyzing*, National Defense Industry Press, Beijing, 2004.

[9] Hu G S, *Digital Signal Processing (Second Edition)*, TsingHua University Press, Beijing, 2003.

[10] L. R. Rabiner, R. W. Schafer, and C. M. Rader, "The Chirp *z*-transform algorithm," *IEEE Trans. on AE*, vol. 17, pp. 86-92, 1969.

[11] R. Roy, T. Kailath, "ESPRIT-Estimation of signal parameters via rotational invariance techniques," *IEEE Trans. on ASSP*, vol. 37, pp. 984-995, 1989.

[12] Petre Stoica, S. Torsten, "Statistical analysis of MUSIC and subspace rotation estimates of sinusoidal frequencies," *IEEE Trans. on ASSP*, vol. 39, pp. 1836-1847, 1991.